HHS Public Access

Author manuscript

Amino Acids. Author manuscript; available in PMC 2022 June 28.

Published in final edited form as:

Amino Acids. 2017 October ; 49(10): 1733–1742. doi:10.1007/s00726-017-2471-9.

Stabilization of Angiotensin-(1–7) by key substitution with a cyclic non-natural amino acid

Anita Wester[1,3],

Marc Devocelle[2],

E. Ann Tallant[3],

Mark C. Chappell[3],

Patricia E. Gallagher[3],

Francesca Paradisi[1,4]

[1]School of Chemistry, University College Dublin, Dublin, Ireland

[2]Department of Pharmaceutical and Medicinal Chemistry, Centre for Synthesis and Chemical Biology, Royal College of Surgeons in Ireland, Dublin, Ireland

[3]Surgery/Hypertension and Vascular Research, Wake Forest School of Medicine, Winston-Salem, NC, USA

[4]School of Chemistry, University of Nottingham, Nottingham, UK

Abstract

Angiotensin-(1–7) [Ang-(1–7)], a heptapeptide hormone of the renin–angiotensin–aldosterone system, is a promising candidate as a treatment for cancer that reflects its anti-proliferative and anti-angiogenic properties. However, the peptide's therapeutic potential is limited by the short half-life and low bioavailability resulting from rapid enzymatic metabolism by peptidases including angiotensin-converting enzyme (ACE) and dipeptidyl peptidase 3 (DPP 3). We report the facile assembly of three novel Ang-(1–7) analogues by solid-phase peptide synthesis which incorporates the cyclic non-natural δ-amino acid ACCA. The analogues containing the ACCA substitution at the site of ACE cleavage exhibit complete resistance to human ACE, while substitution at the DDP 3 cleavage site provided stability against DPP 3 hydrolysis. Furthermore, the analogues retain the anti-proliferative properties of Ang-(1–7) against the 4T1 and HT-1080 cancer cell lines. These results suggest that ACCA-substituted Ang-(1–7) analogues which show resistance against proteolytic degradation by peptidases known to hydrolyze the native heptapeptide may be novel therapeutics in the treatment of cancer.

Francesca Paradisi, Francesca.Paradisi@nottingham.ac.uk.

Compliance with ethical standards

Ethical standards This article does not contain any studies with human participants or animals performed by any of the authors.

Conflict of interest The authors declare that they have no conflict of interest.

Electronic supplementary material The online version of this article (doi:10.1007/s00726-017-2471-9) contains supplementary material, which is available to authorized users.

Keywords

Peptidomimetic; Non-natural amino acid; Angiotensin-(1–7); Angiotensin-converting enzyme; Dipeptidyl peptidase 3; ACCA

Introduction

Angiotensin-(1–7) [Ang-(1–7)] is a heptapeptide hormone of the renin–angiotensin–aldosterone system (RAAS) that mediates its biological effects by activating the G-protein coupled receptor *mas* (Santos et al. 2003). Ang-(1–7) is generated by enzymatic cleavage of the decapeptide Angiotensin I by endopeptidases including neprilysin (NEP) and thimet oligopeptidase and from breakdown of the octapeptide Angiotensin II by carboxypeptidases including angiotensin-converting enzyme 2 (ACE2) and propyl carboxypeptidase (PCP) (Chappell 2016).

Ang-(1–7) was identified as a promising therapeutic for the treatment of cancer based on the anti-proliferative and anti-angiogenic properties of the peptide in models of lung, breast, and prostate cancer (Menon et al. 2007; Soto-Pantoja et al. 2009; Cook et al. 2010; Krishnan et al. 2013a, b; Gallagher et al. 2014). In a mouse model of lung cancer, Ang-(1–7) reduced the growth of human A549 xenograft tumors that was associated with a decrease in cyclooxygenase 2 (COX-2) mRNA and protein (Menon et al. 2007). Attenuation of tumor growth by Ang-(1–7) was also associated with reduced vessel density in the tumors of mice treated with the heptapeptide hormone as compared to saline-treated animals (Soto-Pantoja et al. 2009). The reduction in angiogenesis was associated with a decrease in the proangiogenic protein vascular endothelial growth factor-A (VEGF-A), suggesting that Ang-(1–7) reduces VEGF-A to inhibit angiogenesis (Soto-Pantoja et al. 2009). Ang-(1–7) reduced cell migration and invasion in vitro in A549 human lung cancer cells in association with a decrease in matrix metalloproteinases MMP-2 and MMP-9 expression and activity, suggesting that the heptapeptide hormone may inhibit metastasis (Ni et al. 2012). In two different models of metastatic prostate cancer in the bone, Ang-(1–7) prevented the formation of metastatic tumors, demonstrating the inhibition of metastasis (Krishnan et al. 2013a, b). Furthermore, Ang-(1–7) regulates the tumor microenvironment by inhibiting the proliferation of cancer-associated fibroblasts (CAF) and fibrosis by reducing the mitogen-activated protein kinases (MAPK) ERK1/2 through increasing the MAPK phosphatase DUSP1 in orthotopic breast tumors (Cook et al. 2010). Collectively, these results demonstrate that Ang-(1–7) inhibits proliferation, inflammation, angiogenesis, fibrosis, and metastasis to reduce tumor growth.

Published clinical trials further demonstrate the therapeutic potential of Ang-(1–7) for the treatment of cancer (Petty et al. 2009, 2012; Pham et al. 2013; Rodgers et al. 2006). With limited toxicity and pleiotropic effects on cancer cells and the tumor microenvironment, Ang-(1–7) shows promise as a first-in-class anti-cancer agent (Gallagher et al. 2014). However, a problem commonly associated with peptide therapeutics is their short half-life and limited bioavailability due to rapid degradation by endopeptidases and exopeptidases. Ang-(1–7) is degraded in the circulation by angiotensin-converting enzyme (ACE) resulting

in a short half-life of 29 min (Rodgers et al. 2006). ACE hydrolyzes Ang-(1–7) to the pentapeptide Ang-(1–5) and the dipeptide His^6–Pro^7 (Fig. 1) (Chappell et al. 1998), and ACE inhibitor treatment increases the half-life of Ang(1–7) in the circulation (Chappell 2016). Dipeptidyl peptidase 3 (DPP 3) was recently identified as an enzyme which degrades Ang-(1–7) in the brain, kidney, and human HK-2 renal epithelial cells, and its activity was enhanced in fetal programming (Cruz-Diaz et al. 2016; Marshall et al. 2014a, b). In contrast to ACE, DPP 3 cleaves the first two residues from the N-terminus of Ang-(1–7) to yield Ang-(3–7) which is then rapidly hydrolyzed to Ang-(5–7) (Fig. 1).

The previous attempts to stabilize the heptapeptide hormone for clinical application include encapsulation of the native peptide in the cyclic oligosaccharide cyclodextrin (CyD) [Ang-(1–7)-CyD] (Lula et al. 2007; Fraga-Silva et al. 2011) and in a liposomal delivery system (Silva-Barcellos et al. 2001). Furthermore, a cyclic analogue of Ang-(1–7) was previously shown to be resistant to purified human ACE (Kluskens et al. 2009).

Here, we report the synthesis and biological evaluation of three novel stabilized Ang-(1–7) analogues: ACCA1 **1**, ACCA2 **2,** and ACCA3 **3**. The increase stability to enzymatic degradation was achieved by incorporation of the non-natural δ-amino acid ACCA **4** which was previously employed successfully in dipeptide coupling (O'Reilly et al. 2013). Non-natural amino acids in general and those exhibiting cyclic moieties in particular are valuable building blocks for peptidomimetic synthesis as their incorporation into the sequence of a peptide drug candidate often results in increased stability as recognition by proteolytic enzymes is prevented. Furthermore, rigidity inferred to the usually very flexible peptide structure can lead to enhanced selectivity and efficiency. ACCA **4** was substituted for the native amino acid residues Ile^5 and His^6 to give compounds **1** and **2**, respectively (Fig. 2). Compound **3** (Fig. 2), in which ACCA replaced the Val^3 residue, was also synthesized. The first two peptide analogues target directly the site of hydrolysis by ACE, while the third leaves the ACE hydrolysis site intact and introduces rigidity earlier in the sequence to compare affinity and activity. Compound **3** was also considered to be a potential stable compound as ACCA was substituted at the initial cleavage of site for DPP 3.

The stability of the analogues was assessed against both human ACE and DPP 3. The biological efficacy of the compounds was investigated in cell proliferation assays testing their inhibitory effect on cell growth of 4T1 breast cancer and HT-1080 fibrosarcoma cells.

Results and discussion

Chemistry

The synthesis of ACCA **4** was carried out as previously described (O'Reilly et al. 2013) except for the reduction of the heterocycle double bond which was revised and achieved by transfer hydrogenation (Paryzek et al. 2003). Fmoc protection of ACCA facilitated its use in solid-phase peptide synthesis (Scheme 1). The X-ray crystal structure of **5** visualizes the cyclobutane moiety of the non-natural amino acid and the *cis* orientation of the amino and carboxylic acid group (Fig. 3).

The peptides incorporating ACCA **4** were prepared employing a standard Fmoc/*t*-Bu solid-phase peptide synthesis protocol using an automated peptide synthesizer as described in the experimental procedure. Formation of the peptides was confirmed by MALDI-TOF MS analysis and purification by RP-HPLC generated peptides **1**, **2** and **3** with yields of 64, 46 and 63% yield with >99, >99 and 91% purity, respectively.

Proteolytic stability

Figure 4 shows the HPLC–UV profiles of the Ang-(1–7) standard and the purified ACCA peptides alone (left panels, Fig. 4a, c, e, g) and following a 60 min incubation with human ACE at 37 °C (right panels). As we previously reported (Chappell et al. 1998), ACE catalyzed the metabolism of Ang-(1–7) to the pentapeptide Ang-(1–5) (Fig. 4b). Despite its smaller molecular weight, Ang-(1–5) (20 min) exhibits a greater retention time than Ang-(1–7) (18.3 min) under the current chromatographic conditions. In comparison to Ang-(1–7), the ACCA1 and ACCA2 analogues show complete resistance to ACE metabolism (Fig. 4d, f respectively), while the ACCA3 analogue was metabolized by ACE. Note that intact ACCA3 eluted at 18 min (Fig. 4g) and the ACE-dependent metabolite ACCA3-Ang-(1–5) eluted later at 19.2 min (Fig. 4h).

We then established the extent of metabolism of Ang-(1–7) and the ACCA peptides by human DPP 3 (Fig. 5). As previously reported (Cruz-Diaz et al. 2016), DPP 3 ultimately metabolizes Ang-(1–7) (Fig. 5a) to the tripeptide Ile^5–His^6–Pro^7 or Ang-(5–7) that elutes at 8 min (Fig. 5b). This profile reflects the initial metabolism of Ang-(1–7) to the dipeptide Asp^1–Arg^2 and Ang-(3–7) followed by the more rapid hydrolysis of Ang-(3–7) to Val^3–Tyr^4 and Ang-(5–7) which accounts for the major peak of Ang-(5–7) in the chromatograph. Figure 5d demonstrates that ACCA1 (Fig. 5c) is metabolized by DPP 3 to ACCA1-(3–7) (6.2 min). It is possible that the 2.8 min peak is ACCA1(5–7); however, the ACCA substitution of Ile^5 may prevent the hydrolysis of ACCA1-(3–7) by DPP 3 and the 2.8 min peak may not represent a metabolite of ACCA1. In comparison, ACCA2 (Fig. 5e) is metabolized by DPP 3 to the tripeptide ACCA2-(5–7) (Fig. 5f). In this case, substitution of His^6 with the ACCA residue may allow for more complete metabolism of the ACCA2-(3–7) peptide following the initial hydrolysis of ACCA2 (see pathway). In contrast, the ACCA3 analogue (Fig. 5g), where the Val^3 residue is replaced, is resistant to the initial hydrolysis step by DPP 3 (Fig. 5h).

Cell growth

Murine 4T1 breast cancer cells and human HT-1080 fibrosarcoma cells were incubated with one of the three ACCA analogues or Ang-(1–7), to preliminary assess whether the modified peptides inhibited cell proliferation similar to the parent compound Ang-(1–7). 4T1 cells closely mimic human triple negative breast cancer cells and HT-1080 cells are human sarcoma cells. Ang-(1–7) (100 nM) served as the control and was added daily, as it is rapidly degraded. ACCA1, ACCA2, or ACCA3 was added as a single aliquot on day 0, at either a concentration of 100 nM or 1 μM, and the total number of cells per well was counted after 3 or 4 days. The Ang-(1–7)-ACCA analogues did not require further additions for the duration of the study. ACCA, and a range of ACCA dipeptides, did not show any toxicity on C6 glioma cell lines up to 200 μM, significantly higher than the concentrations used in this

study (Pes 2013). As shown in Fig. 6, 100 nM Ang-(1–7) reduced proliferation of the mouse triple negative breast cancer cells by 34% compared to the untreated control cells. ACCA1 significantly reduced proliferation at the single treatment dose of 1 μM, but a tenfold lower dose was not effective. In contrast, ACCA2 and ACCA3 significantly reduced proliferation of the 4T1 cells at both single doses 100 nM and 1 μM. The growth of HT-1080 sarcoma cells was reduced 44% by 100 nM Ang(1–7) that was again added daily as compared to the control (Fig. 7). Although ACCA2 did not reduce the growth of HT-1080 cells, both ACCA1 and ACCA3 reduced proliferation at single doses of 1 μM.

Conclusion

The present study is the first to explore key substitutions with a non-natural amino acid as a strategy for stabilizing Ang-(1–7) against degradation by both ACE and DPP 3. ACCA is a non-functionalized amino acid which offers structural rigidity without introducing additional reactivity. The advantage of this approach is the ease of synthesis of the desired targets that can be accomplished by standard solid-phase protocols, as well as the possibility that the introduction of additional structural modifications will further optimize the stability and activity of the peptide.

Our study of the three ACCA substitutions at various positions within Ang-(1–7) structure indicated differential sensitivities of the three analogues to hydrolysis by ACE and DPP 3. When ACCA is substituted for the two native amino acid residues at the Ile^5–His^6 site of ACE hydrolysis, it confers to the peptide significant resistance to ACE enzymatic degradation, but only limited or no protection from DPP 3 hydrolysis which is consistent with the catalytic preference of the aminopeptidase. However, the opposite effect was observed when ACCA replaced Val^3; the peptide was hydrolyzed by ACE to a similar extent as Ang-(1–7) but showed resistance to degradation by DPP 3 The ACCA substitution at Ile^5 may allow for the initial hydrolysis to ACCA1-(3–7), but could potentially prevent the subsequent hydrolysis step to generate ACCA1-(5–7) by the aminopeptidase. Additional studies are necessary to fully elucidate the hydrolysis profile of the ACCA1 **1** analogue by DPP 3.

Preliminary tests on two cancer cell lines which respond to the anti-proliferative effects of Ang-(1–7) (4T1 and HT-1080) were also carried out on the synthesized analogues. All three Ang-(1–7)-ACCA analogues significantly reduced cell growth of the 4T1 breast cancer cells by approximately 25% at the single dose of 1 μM, that was comparable to the extent of inhibition with 100 nM Ang(1–7) (repeated daily dosage) after 4 days. In contrast, ACCA1 **1** and ACCA3 **3** were significantly more active than ACCA2 **2** with HT-1080 cells (growth reduction by 40–50% and ~20%, respectively), also comparable to Ang-(1–7). Metabolism of Ang-(1–7) or the Ang-(1–7)-ACCA analogues in either cell line is not currently known and it is possible that ACCA2 is more susceptible to degradation by other peptidases expressed in the HT-1080 cells. While this study is preliminary, it offers significant opportunities to further explore these types of modification to the Ang-(1–7) peptide structure. Future studies will focus on expanding the cell lines tested, and degradation pathways for Ang-(1–7) and the Ang-(1–7)-ACCA analogues will be performed. Nevertheless, our results clearly demonstrate that the ACCA-substituted Ang-(1–

7) analogues retain the anti-proliferative properties of the native peptide while exhibiting enhanced enzymatic stability. The successful synthesis of these peptidase-resistant and bioactive analogues suggests that ACCA-substituted Ang-(1–7) may reduce tumor growth as well as have the therapeutic potential for use in other cardiovascular pathologies.

Experimental section

Non-natural amino acid synthesis—Fmoc-OSu was purchased from Iris Biotech. Li^+ pellets were purchased from Fluka. Ammonia was purchased from BOC gases. All other reagents and solvents were purchased from Sigma-Aldrich and used without further purification. Anhydrous CH_2Cl_2 and THF were obtained from a Puresolv-EN™ solvent purification system. When necessary, reactions were performed under inert atmosphere of nitrogen, using oven dried glassware. Oxygen-free nitrogen was obtained from BOC gases and used without further drying. NMR spectra were recorded on Varian VNMRS 300, 400, and 500 MHz instruments at 25 °C. Tetramethylsilane was used as an internal standard. The coupling constants (J) are in hertz (Hz) and the chemical shifts (δ) are in parts per million (ppm). Signals were assigned with the aid of COSY, HSQC, and HMBC spectra. High-resolution mass spectra were recorded using electron spray ionization (ESI) on a Waters Micromass LCT (MeOH/H_2O, 60:40) TOF instrument with a cone voltage of 35 V and a capillary voltage of 3000 V and are reported in the form m/z (intensity relative to base = 100). Infrared spectra were recorded on a Bruker ALPHA Platinum ATR spectrometer and melting points were determined on a Stuart™ SMP10 melting point apparatus. Crystal data were collected using a Rigaku Oxford Diffraction SuperNova A diffractometer fitted with an Atlas detector. Evaporation in vacuo refers to the removal of solvent on a Büchi rotary evaporator with an integrated vacuum pump. Compounds were purified by flash chromatography using D avisil® Chromatographic silica media (40–63 μm) or ion-exchange chromatography using a DOWEX® 50WX8 resin (100–200 mesh, SigmaAldrich). Thin-layer chromatography (TLC) was carried out on aluminum sheets pre-coated with silica gel 60 F_{254} (Merck) and compounds were visualized by UV or by treatment with potassium permanganate stain (0.75 g $KMnO_4$, 5 g K_2CO_3, and 0.625 mL 10% (w/v) NaOH in 100 mL H_2O) or ninhydrin stain (1.5 g ninhydrin and 3 mL AcOH in 100 mL *n*-butanol) followed by heating.

***N*-(9-Fluorenylmethoxycarbonyl)-*cis*-3-(aminomethyl) cyclobutane carboxylic acid (5)—**ACCA **4** (101 mg, 0.78 mmol, 1.0 eq.) was dissolved in 10% (w/v) aq. Na_2CO_3 (2.1 mL, 1.95 mmol, 2.5 eq.), 1,4-dioxane (5 mL) was added, and the reaction was cooled to 0 °C. Fmoc-OSu (395 mg, 1.17 mmol, 1.5 eq. in 1,4-dioxane (2.5 mL) was added and the mixture was stirred for 45 min at 0 °C and for 1 h at room temperature). The reaction mixture was then washed with Et_2O (30 mL). The aqueous layer was acidified with 1 M HCl and extracted with EtOAc (4 × 25 mL). The combined organic layers were washed with brine, dried over Na_2SO_4, filtered, and concentrated in vacuo. The crude material was purified by silica gel column chromatography (cyclohexane/EtOAc, from 95:5 to 40:60) and crystallized from acetone and petroleum sprits (b.p. 40–60 °C) to give the product (260 mg, 95%) as a white solid: R_f = 0.36 (cyclohexane/EtOAc, 1:5); m.p. 134–135 °C; ^1H NMR (500 MHz, ($CD_3)_2CO$) δ = 7.71–7.70 (m, 2H, Ar), 7.54–7.53 (m, 2H, Ar), 7.27–7.16 (m, 4H, Ar), 6.41 (s, 1H, NH), 4.18 (d, J = 7.2 Hz, 2H, C=OOCH_2), 4.08–4.05 (m, 1 H,

C=OOCH$_2$C*H*), 3.05–3.02 (m, 2H, N CH$_2$), 2.91–2.83 (m, 1H, C*H*C=OOH), 2.38–2.29 (m, 1H, NCH$_2$C*H*), 2.15–2.09 (m, 2H, C=OCH(C*H*H)$_2$), 1.88–1.82 (m, 2H, C=OCH(CH*H*)$_2$); ^{13}C NMR (126 MHz, C D$_3$OD) δ = 175.4, 156.4, 144.3, 141.2, 127.6, 127.0, 125.2, 119.9, 65.9, 47.2, 45.7 33.5, 31.2, 28.5; ν_{max} (neat) = 1709, 1690 cm^{-1}; HRMS (ES) *m/z* = 374.1377 [M + Na]$^+$ $C_{21}H_{21}NO_4Na$ requires 374.1368.

Peptide synthesis, purification, and characterization—SPPS was carried out on a 0.1 mmol scale. Amino acids were purchased Fmoc protected (Iris Biotech) with Trt as side-chain protecting group for His, Pbf for Arg, and *t*-Bu for Tyr and Asp. The polystyrene resin (1% DVB crosslinks, particle size: 100–100 mesh, loading: 0.52 mmol/g) was purchased with a 2-chlorotrityl (2CT) linker preloaded with the proline residue (Iris Biotech). HATU (Iris Biotech) was employed as the coupling reagent and DIPEA (Sigma-Aldrich) as the base. All other reagents and solvents were purchased from Sigma-Aldrich and used without further purification. Peptide synthesis was carried out using an automated peptide synthesizer (Applied Biosystems 433A) in the Royal College of Surgeons in Ireland (RCSI). Single coupling cycles (except for the amino acid coupling to the resin-bound proline and double coupling cycle) using a tenfold excess of Fmoc protected amino acid to resin substitution were carried out employing HATU/DIPEA coupling chemistry in NMP (Thermo Fisher Scientific). Fmoc cleavage was monitored with a PerkinElmer Series 200 inline spectrophotometer and the UV absorbance was detected at 301 nm. Peptide cleavage from the resin and side-chain deprotection was achieved by gentle stirring in a mixture of 87.5% TFA, 5% H $_2$O, 5% thioanisole, and 2.5% triisopropylsilane for 2.5 h at room temperature. The volume of the TFA and scavenger mixture was reduced by half under a stream of nitrogen and the peptide was precipitated by the addition of cold ether. Precipitation from the full volume of the cleavage cocktail had been attempted but was found not to be possible. The suspension was centrifuged for 5 min at 8000 rpm, the supernatant was decanted, and the peptides were re-suspended in ether. This step was repeated three times. The peptides were then air dried, dissolved in double distilled water, and lyophilized to give the crude material as white solids. Chromatographic purification was performed on a Shimadzu Prominence HPLC using an Aeris Peptide column (3.6 μm XB-C18 4.6 mm × 150 mm; Phenomenex, Torrance CA). 0.1% phosphoric acid (Sigma, Chicago IL) in Milli-Q water (Millipore Systems, Billerica MA) was employed as mobile phase A and 80% acetonitrile/0.1% phosphoric acid as mobile phase B with a linear gradient of 0–15% B in 20 min, 15–35% B in 10 min, and 35% isocratic for 5 min at a flow rate of 1 mL/min at room temperature. The UV absorbance was detected at 220 nm with an inline spectrophotometer. The peptide peaks were collected and completely evaporated in a vacuum centrifuge. MALDI-TOF MS spectra were acquired in Trinity College Dublin using a Waters MALDI Q-TOF Premier. The instrument was operated in positive or negative modes as required. Laser energy was provided by a N_2 laser operating at 337 nm. Samples were mixed with a CHCA (*α*-cyano-4-hydroxycinnamic acid) matrix. 1 μL of the matrix/sample solutions were loaded onto a MALDI plate and allowed to air dry. The instrument was calibrated using PEG. The internal lock mass used was [Glu] Fibrinopeptide B. MassLynx 4.1 software was used to carry out the analysis.

ACCA1 (**1**) H-Asp-Arg-Val-Tyr-ACCA-His-Pro-OH: white solid, yield = 64, >99% purity, R_t = 14.5 min; MALDI-TOF MS (*m/z*) = 897.4580 $[M + H]^+$ $C_{41}H_{61}N_{12}O_{11}$ requires 897.4583.

ACCA2 (**2**) H-Asp-Arg-Val-Tyr-Ile-ACCA-Pro-OH: white solid, yield = 46, >99% purity, R_t = 25.8 min; MALDI-TOF MS (*m/z*) = 873.4827 $[M + H]^+$ $C_{41}H_{65}N_{10}O_{11}$ requires 873.4834.

ACCA3 (**3**) H-Asp-Arg-ACCA-Tyr-Ile-His-Pro-OH: white solid, yield = 63, 91% purity, R_t = 18.11 min; MALDI-TOF MS (*m/z*) = 911.4763 $[M + H]^+$ $C_{42}H_{63}N_{12}O_{11}$ requires 911.4739.

Proteolytic stability

The stability of the three purified ACCA analogues was assessed against human ACE and DPP 3. The angiotensin standards Ang-(1–7) and Ang-(1–5) were obtained from Bachem (Torrance, CA). The purified analogues or Ang(1–7) (100 nmol) were incubated with human ACE (1.0 μg, R&D Systems, Minneapolis, MN) or human DPP 3 (0.1 μg, R&D Systems) for 60 min at 37 °C in 0.1 mL of the HEPES assay buffer (25 mM HEPES, 125 mM NaCl, 10 μM Z nCl_2, pH 7.5), and the assays were terminated with 1.0% phosphoric acid. The purity of each compound and the extent of peptide metabolism by ACE or DPP 3 were assessed with the Shimaduz Prominence HPLC system equipped with a narrow-bore Aeris Peptide XB-C18 (2.0 × 100 mm, Phenomenex) using identical gradient conditions described above and the UV profile was monitored at 220 nm.

Cell culture

Murine breast cancer cells (4T1; ATCC CRL-2539) were derived from a spontaneously arising tumor in the mammary tissue of a BALB-c mouse. Human fibrosarcoma cells (HT-1080; ATCC CCL-121) were derived from a fibrosarcoma from a 35-year-old male. 4T1 cells were grown in RPMI media with 10% fetal bovine serum (FBS), 10 nmol/L HEPES, 100 μg/mL penicillin, and 100 U/mL streptomycin, while HT-1080 cells were grown in EMEM with 10% FBS, 10 nmol/L HEPES, 100 μg/mL penicillin, and 100 U/mL streptomycin. Cells were maintained at 37 °C in a humidified atmosphere of 5% CO_2.

Cell growth

4T1 cells or HT-1080 cells were seeded into 24-well cluster plates and allowed to grow overnight, in 10% FBS. After 24 h, the FBS was reduced to 1% and the rapidly proliferating cells were incubated with 100 nM Ang-(1–7) as previously described (Cook et al. 2010; Gallagher and Tallant 2004; Krishnan et al. 2013b), added daily, or either 100 nM or 1 μM ACCA1, ACCA2, or ACCA3 for 3 or 4 days. The total number of cells per well was counted using a Nexelcom Cellometer and compared to the control.

Statistical analysis

The data were analyzed using GraphPad Prism 5 software and results are displayed as the mean ± standard error of the mean (SEM) of at least three independent experiments (n = 3) measured in triplicate, unless otherwise stated. Statistical analysis was by one-way ANOVA

followed by Dunnett's multiple comparison test. Values of $p < 0.05$ were considered significant; * denotes $p < 0.05$, ** denotes $p < 0.01$, and *** denotes $p < 0.001$.

Supplementary Material

Refer to Web version on PubMed Central for supplementary material.

Acknowledgements

We would like to thank the National University of Ireland for funding this research. We would like to acknowledge the facilities in the Centre for Synthesis and Chemical Biology (CSCB), funded by the Higher Education Authority's Programme for Research in Third Level Institutions (PRTLIs). We are grateful to Dr. Helge Müller-Bunz for his work on the X-ray crystal structure. We would also like to acknowledge the Science Foundation Ireland Equipment Grant 06/RFP/CHO024/EC07, the National Institutes of Health (NIH) HD084227, the American Heart Association Grants AHA-151521 and AHA-355741, the Randi B. Weiss Cancer Research Fund (Winston-Salem, NC), and the Farley-Hudson Foundation (Jacksonville, NC). Finally, we acknowledge the technical expertise of Nancy T. Pirro for the peptide metabolism studies and L. Tenille Howard for cell proliferation studies.

Abbreviations

ACCA	*cis*-3-(Aminomethyl)cyclobutanecarboxylic acid
ACE	Angiotensin-converting enzyme
HATU	*N*-[(Dimethylamino)-1*H*-1,2,3-triazolo-[4,5-*b*]pyridin-1-ylmethylene]-*N*-methylmethanaminium hexafluorophosphate *N*-oxide
HEPES	4-(2-Hydroxyethyl)-1-piperazineethanesulfonic acid
HPLC	High-performance liquid chromatography
HRMS	High-resolution mass spectrometry
2CT resin	2-Chlorotrityl resin
NMP	*N*-methylpyrrolidone
DIPEA	*N,N*-Diisopropylethylamine
DPP 3	Dipeptidyl peptidase 3
Fmoc	9-Fluorenylmethoxycarbonyl
Fmoc-OSu	*N*-(9-Fluorenylmethoxycarbonyloxy) succinimide
Pbf	2,2,4,6,7-Pentamethyldihydrobenzyofuran-5-sulfonyl
***t*-Bu**	*t*-Butyl
Trt	Trityl
TFA	Trifluoroacetic acid
SPPS	Solid-phase peptide synthesis

References

Chappell MC (2016) Biochemical evaluation of the renin-angiotensin system: the good, bad, and absolute? Am J Physiol Heart Circ Physiol 310:H137–H152 [PubMed: 26475588]

Chappell MC, Pirro NT, Sykes A, Ferrario CM (1998) Metabolism of angiotensin-(1–7) by angiotensin-converting enzyme. Hypertension 31:362–367 [PubMed: 9453329]

Cook KL, Metheny-Barlow LJ, Tallant EA, Gallagher PE (2010) Angiotensin-(1–7) reduces fibrosis in orthotopic breast tumors. Cancer Res 70:8319–8328 [PubMed: 20837666]

Cruz-Diaz N, Wilson BA, Pirro NT, Brosnihan KB, Marshall AC, Chappell MC (2016) Identification of dipeptidyl peptidase 3 as the angiotensin-(1–7) degrading peptidase in human HK-2 renal epithelial cells. Peptides 83:29–37 [PubMed: 27315786]

Fraga-Silva RA, Costa-Fraga FP, De Sousa FB, Alenina N, Bader M, Sinisterra RD, Santos RA (2011) An orally active formulation of angiotensin-(1–7) produces an antithrombotic effect. Clinics 66:837–841 [PubMed: 21789389]

Gallagher PE, Tallant EA (2004) Inhibition of human lung cancer cell growth by angiotensin-(1–7). Carcingenesis 25:2045–2052

Gallagher PE, Arter AL, Deng G, Tallant EA (2014) Angiotensin-(1–7): a peptide hormone with anti-cancer activity. Curr Med Chem 21:2417–2423 [PubMed: 24524765]

Kluskens LD, Nelemans SA, Rink R, de Vries L, Meter-Arkema A, Wang Y, Walther T, Kuipers A, Moll GN, Haas M (2009) Angiotensin-(1–7) with thioether bridge: an angiotensin-converting enzyme-resistant, potent angiotensin-(1–7) analog. J Pharmacol Exp Ther 328:849–854 [PubMed: 19038778]

Krishnan B, Smith TL, Dubey P, Zapadka ME, Torti FM, Willingham MC, Tallant EA, Gallagher PE (2013a) Angiotensin-(1–7) attenuates metastatic prostate cancer and reduces osteoclastogenesis. Prostate 73:71–82 [PubMed: 22644942]

Krishnan B, Torti FM, Gallagher PE, Tallant EA (2013b) Angiotensin-(1–7) reduces proliferation and angiogenesis of human prostate cancer xenografts with a decrease in angiogenic factors and an increase in sFlt-1. Prostate 73:60–70 [PubMed: 22644934]

Lula I, Denadai ÂL, Resende JM, de Sousa FB, de Lima GF, PiloVeloso D, Heine T, Duarte HA, Santos RAS, Sinisterra RD (2007) Study of angiotensin-(1–7) vasoactive peptide and its β-cyclodextrin inclusion complexes: complete sequence-specific NMR assignments and structural studies. Peptides 28:2199–2210 [PubMed: 17904691]

Marshall AC, Pirro NT, Rose JC, Diz DI, Chappell MC (2014a) Evidence for an angiotensin-(1–7) neuropeptidase expressed in the brain medulla and CSF of sheep. J Neurochem 130:313–323 [PubMed: 24661079]

Marshall AC, Shaltout HA, Pirro NT, Rose JC, Diz DI, Chappell MC (2014b) Enhanced activity of an angiotensin-(1–7) neuropeptidase in glucocorticoid-induced fetal programming. Peptides 52:74–81 [PubMed: 24355101]

Menon J, Soto-Pantoja DR, Callahan MF, Cline JM, Ferrario CM, Tallant EA, Gallagher PE (2007) Angiotensin-(1–7) inhibits growth of human lung adenocarcinoma xenografts in nude mice through a reduction in cyclooxygenase-2. Cancer Res 67:2809–2815 [PubMed: 17363603]

Ni L, Feng Y, Wan H, Ma Q, Fan L, Qian Y, Li Q, Xiang Y, Gao B (2012) Angiotensin-(1–7) inhibits the migration and invasion of A549 human lung adenocarcinoma cells through inactivation of the PI3K/Akt and MAPK signaling pathways. Oncol Rep 27:783–790 [PubMed: 22089256]

O'Reilly E, Pes L, Ortin Y, Müller-Bunz H, Paradisi F (2013) Synthesis of a conformationally constrained δ-amino acid building block. Amino Acids 44:511–518 [PubMed: 22851051]

Paryzek Z, Koenig H, Tabaczka B (2003) Ammonium formate/palladium on carbon: a versatile system for catalytic hydrogen transfer reductions of carbon-carbon double bonds. Synthesis 2003:2023–2026

Pes L (2013) Study of the non proteinogenic delta-amino acid ACCA, its biological investigation and application. PhD thesis, University College Dublin

Petty WJ, Miller AA, McCoy TP, Gallagher PE, Tallant EA, Torti FM (2009) Phase I and pharmacokinetic study of angiotensin-(1–7), an endogenous antiangiogenic hormone. Clin Cancer Res 15:7398–7404 [PubMed: 19920106]

Petty WJ, Aklilu M, Varela VA, Lovato J, Savage PD, Miller AA (2012) Reverse translation of phase I biomarker findings links the activity of angiotensin-(1–7) to repression of hypoxia inducible factor-1alpha in vascular sarcomas. BMC Cancer 12:404 [PubMed: 22963500]

Pham H, Schwartz BM, Delmore JE, Reed E, Cruickshank S, Drummond L, Rodgers KE, Peterson KJ, di Zerega GS (2013) Pharmacodynamic stimulation of thrombogenesis by angiotensin (1–7) in recurrent ovarian cancer patients receiving gemcitabine and platinum-based chemotherapy. Cancer Chemother Pharmacol 71:965–972 [PubMed: 23370663]

Rodgers KE, Oliver J, di Zerega GS (2006) Phase I/II dose escalation study of angiotensin 1–7 [A(1–7)] administered before and after chemotherapy in patients with newly diagnosed breast cancer. Cancer Chemother Pharmacol 57:559–568 [PubMed: 16096787]

Santos RAS, Silva ACS, Maric C, Silva DMR, Machado RP, de Buhr I, Heringer-Walther S, Pinheiro SVB, Lopes MT, Bader M, Mendes EP, Lemos VS, Campagnole-Santos MJ, Schultheiss H-P, Speth R, Walther T (2003) Angiotensin-(1–7) is an endogenous ligand for the G protein-coupled receptor Mas. Proc Natl Acad Sci U S A 100:8258–8263 [PubMed: 12829792]

Silva-Barcellos NM, Frézard F, Caligiorne S, Santos RAS (2001) Long-lasting cardiovascular effects of liposome-entrapped angiotensin-(1–7) at the rostral ventrolateral medulla. Hypertension 38:1266–1271 [PubMed: 11751701]

Soto-Pantoja DR, Menon J, Gallagher PE, Tallant EA (2009) Angiotensin-(1–7) inhibits tumor angiogenesis in human lung cancer xenografts with a reduction in vascular endothelial growth factor. Mol Cancer Ther 8:1676–1683 [PubMed: 19509262]

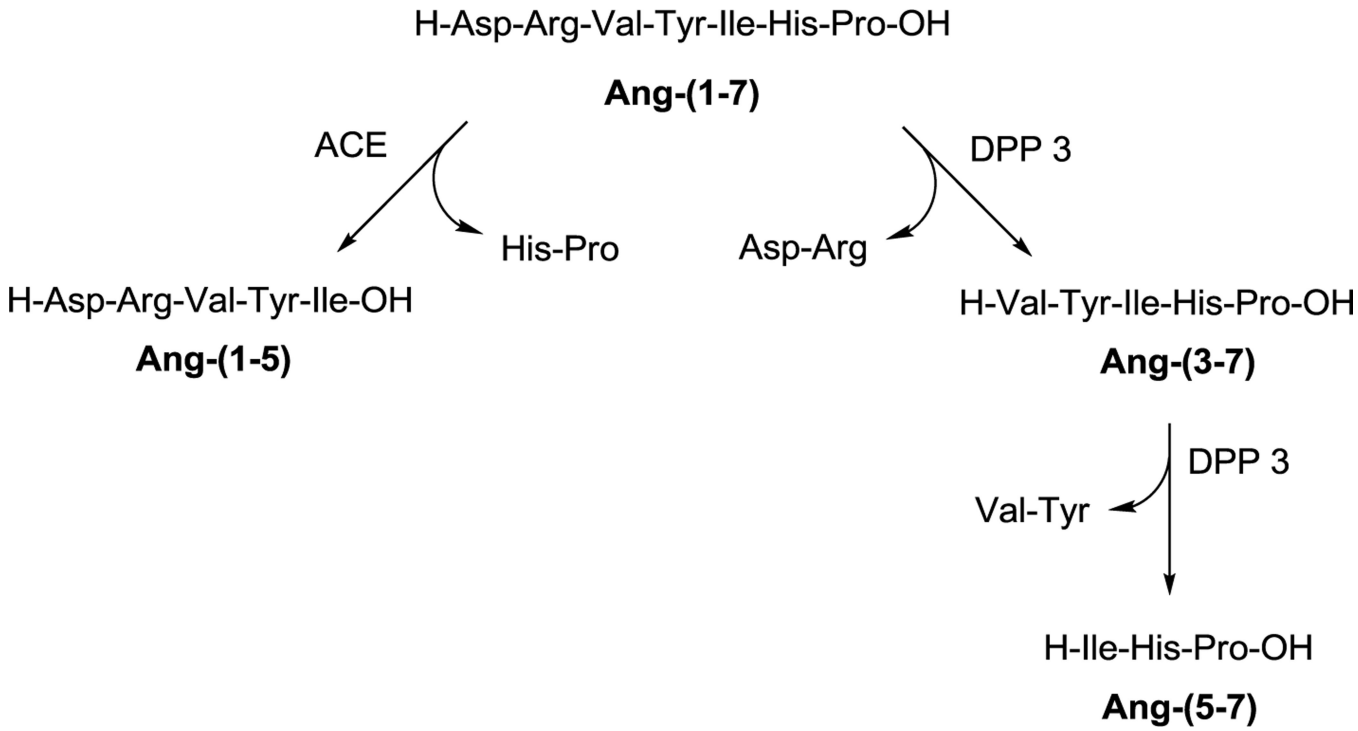

Fig. 1.

Proteolytic cleavage of angiotensin-(1–7) by angiotensin-converting enzyme (ACE) and dipeptidyl peptidase 3 (DPP 3)

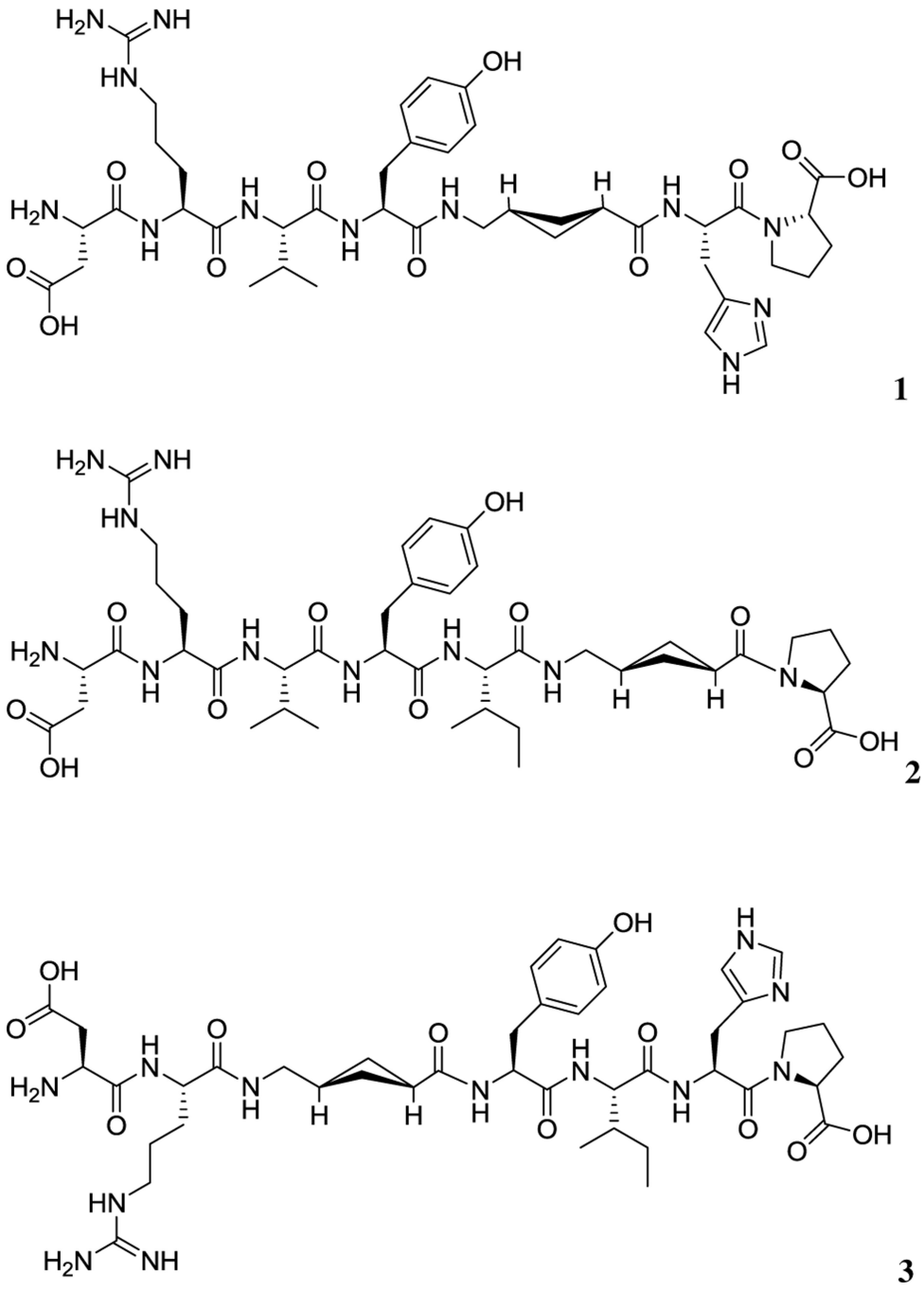

Fig. 2.
Structures of the Ang-(1–7) analogues ACCA1 **1**, ACCA2 **2,** and ACCA3 **3**

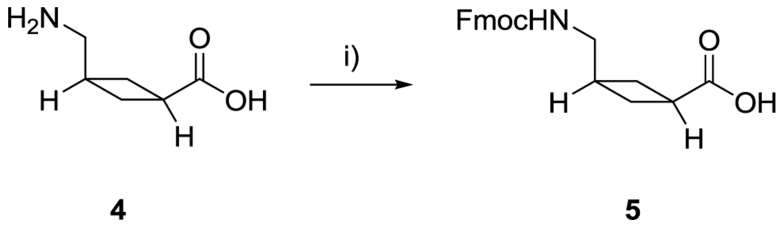

4 **5**

Scheme 1.

Synthesis of Fmoc-ACCA 5. *i*) Fmoc-OSu (1.5 eq.), 10% (w/v) aq. Na_2CO_3, dioxane, 0 °C—r.t., 1 h 45 min, 95%

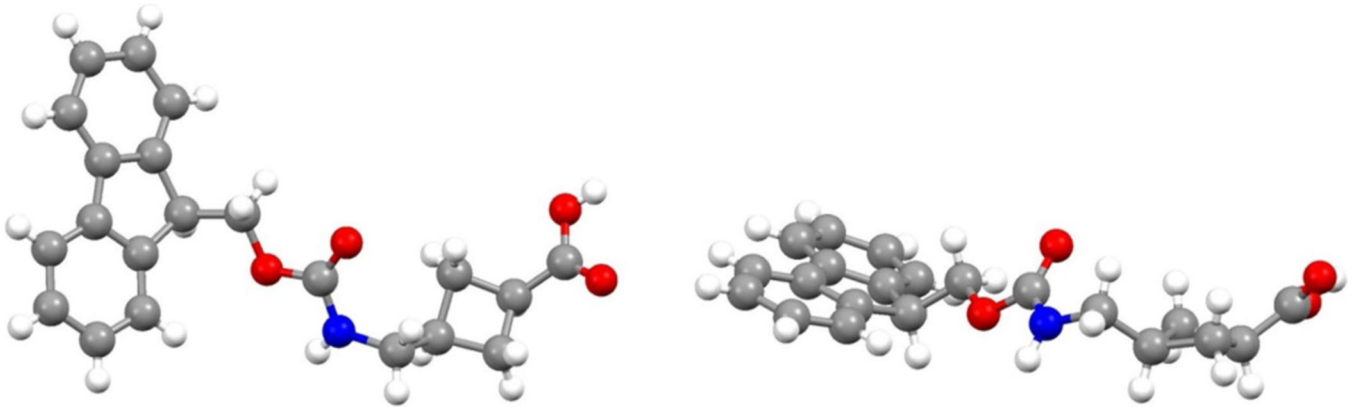

Fig. 3.
Two orientations of the X-ray crystal structure of Fmoc-ACCA **5** (CCDC 1514790)

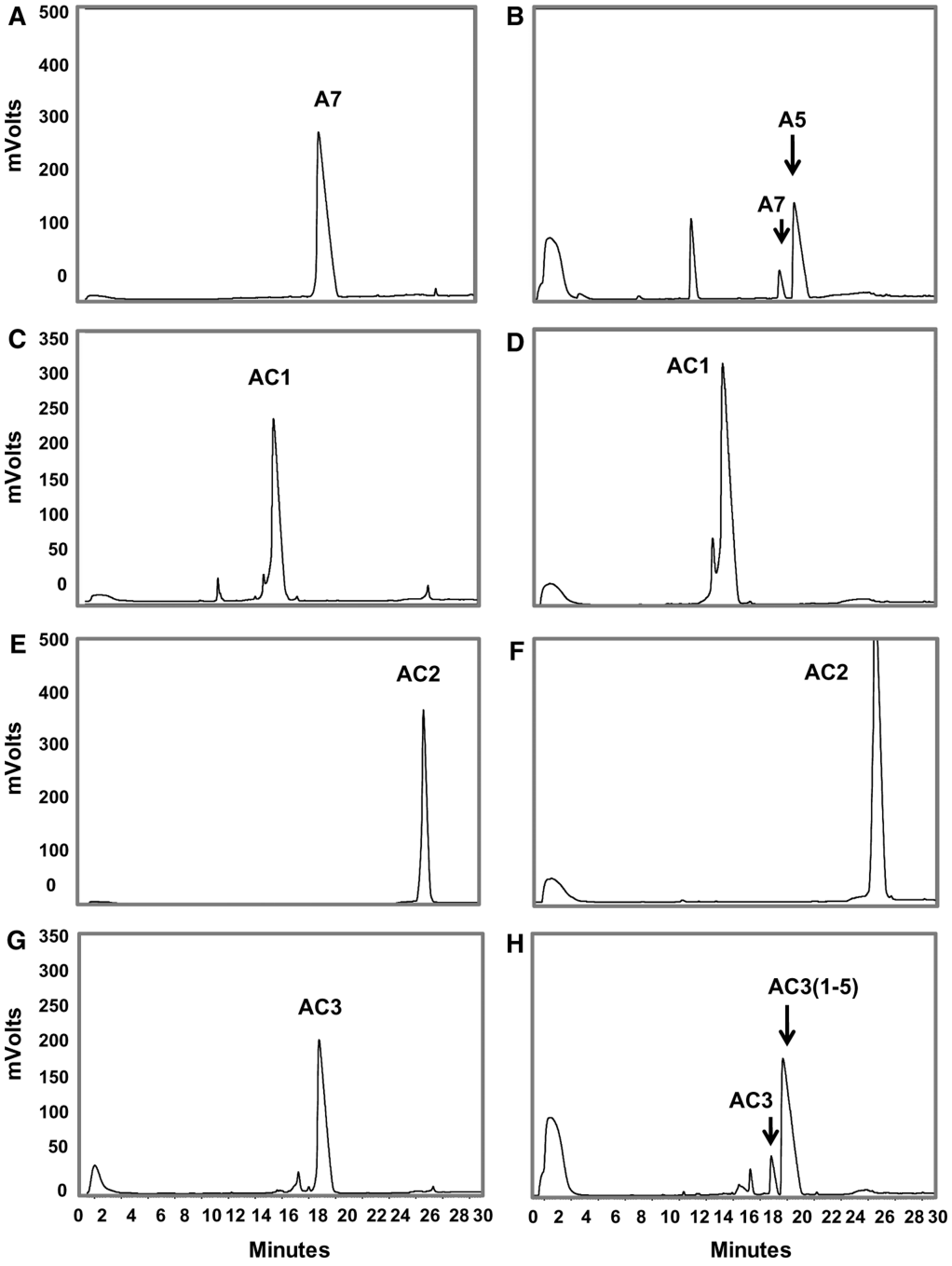

Fig. 4.

HPLC–UV profile of the ACCA peptides and following exposure to ACE. **a** Ang-(1–7) (A7) standard. **b** ACE metabolizes Ang(1–7) to Ang-(1–5) (A5). **c** ACCA1 (AC1) standard. **d** ACCA1 is not metabolized by ACE. **e** ACCA2 (AC2) standard. **f** ACCA2 is not metabolized by ACE. **g** ACCA3 (AC3) standard. **h** ACCA3 (AC3) is metabolized by ACE to ACCA3-(1–5) [AC3(1–5)]

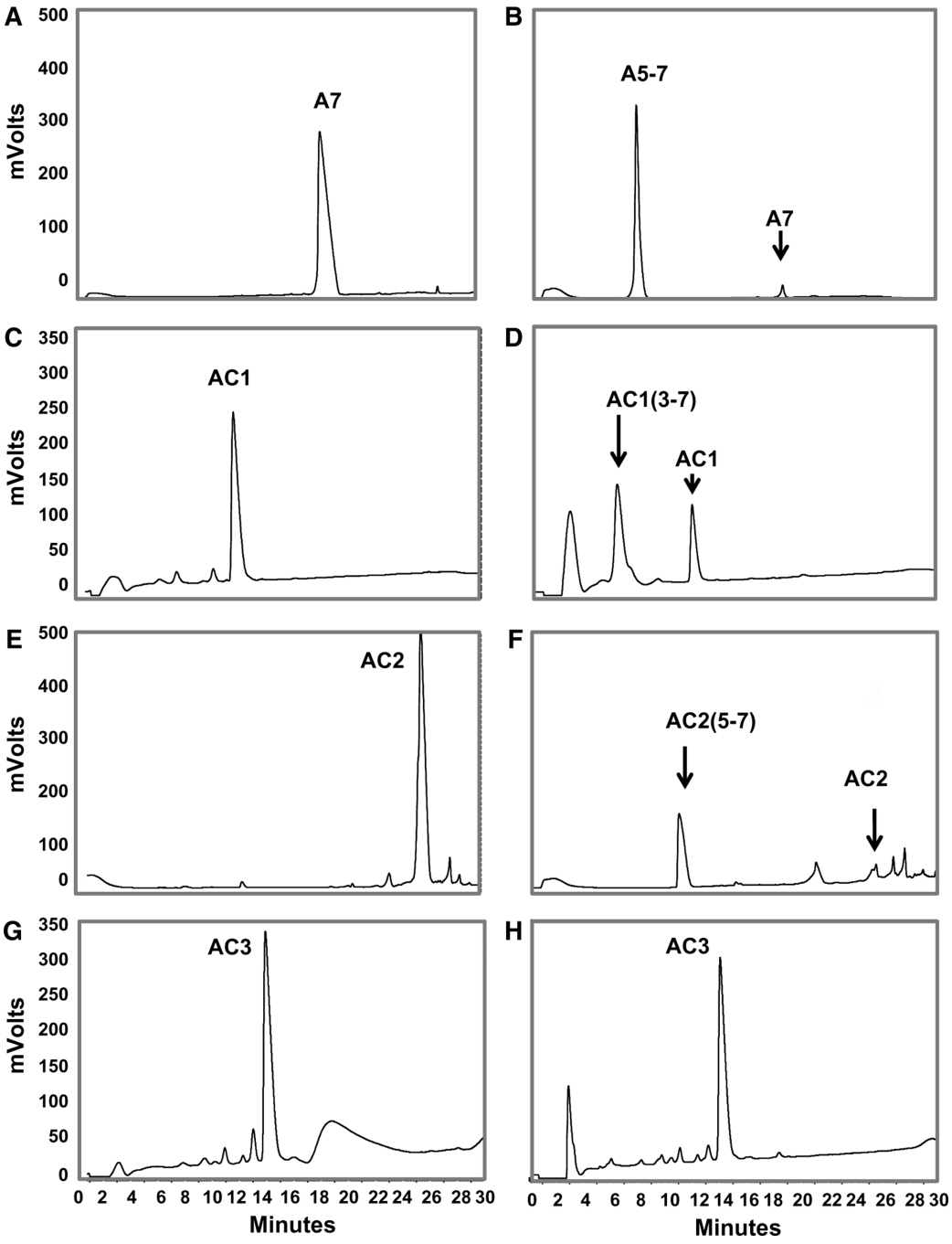

Fig. 5.

HPLC–UV profile of the ACCA peptides and following exposure to DPP 3. **a** Ang-(1–7) (A7) standard. **b** DPP 3 metabolizes Ang-(1–7) to Ang-(3–7) and ultimately to Ang-(5–7) (A5–7). **c** ACCA1 (AC1) standard. **d** ACCA1 is metabolized by DPP 3 to likely ACCA1-(3–7) [AC1(3–7)], eluting at 6.2 min. **e** ACCA2 (AC2) standard. **f** ACCA2 is likely degraded fully to ACCA2-(5–7) [AC2 (5–7)]. **g** ACCA3 (AC3) standard. **h** ACCA3 is more stable to DPP 3 hydrolysis in comparison to Ang-(1–7) and the other analogues

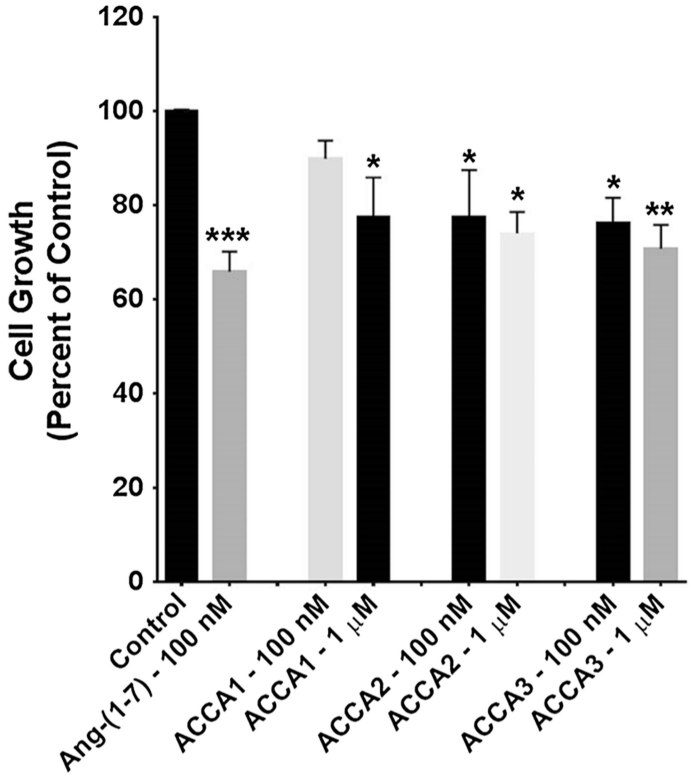

Fig. 6.

Effect of Ang-(1–7) or each of the Ang-(1–7)-ACCA analogues on the proliferation of 4T1 murine triple negative breast cancer cells. Ang-(1–7) (100 nM) was added daily to rapidly growing cells, while each of the ACCA analogues was added once to rapidly growth cells at day 0. The total cell number per well was counted after 3–4 days. $n = 4–5$ in triplicate; *$p < 0.05$, **$p < 0.01$, and ***$p < 0.001$

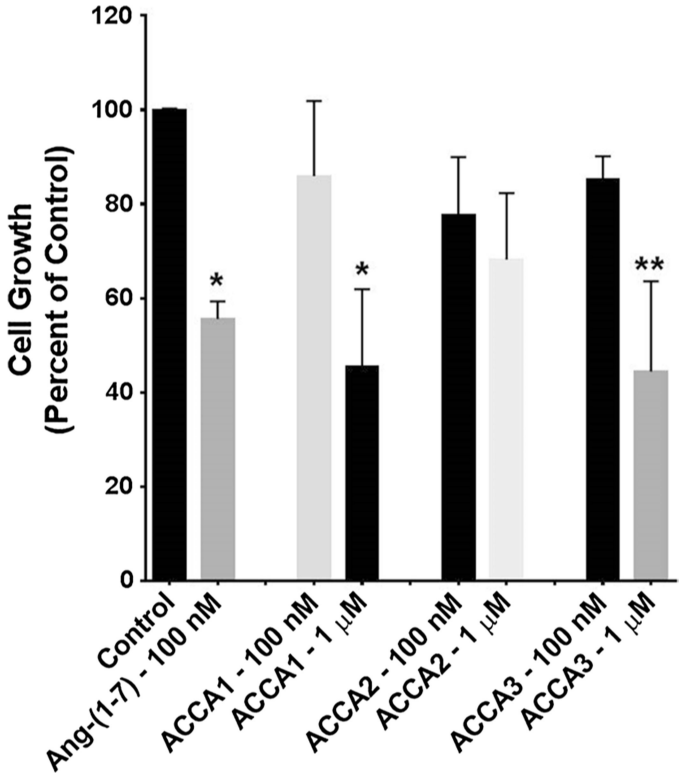

Fig. 7.

Effect of Ang-(1–7) or each of the Ang-(1–7)-ACCA analogues on the proliferation of HT-1080 human sarcoma cells. Ang(1–7) (100 nM) was added daily to rapidly growing cells, while each of the ACCA analogues was added once to rapidly growth cells at day 0. The total cell number per well was counted after 3–4 days. $n = 4–5$ in triplicate; *$p < 0.05$ and **$p < 0.01$